Experiments of a Space Robot in the Free-Fall Environment

Yasuyuki Watanabe
National Space Development Agency of Japan
Tsukuba Space Center, 1-1, Sengen 2-chome, Tsukuba-city, Ibaraki 305-8505 Japan
phone: +81-298-59-2967, fax: +81-298-52-2410, e-mail: Watanabe.Yasuyuki@nasda.go.jp

Yoshihiko Nakamura
Department of Mechano-Informaics, University of Tokyo
3-1, Hongo 7-chome, Bunkyo-ku, Tokyo 113-8656 Japan
phone: +81-3-5804-6256, fax: +81-3-3818-0835, e-mail: nakamura@ynl.t.u-okyo.ac.jp

Abstract

We propose an experimental system of a space robot in the microgravity environment at the Japan Microgravity Center (JAMIC), where the microgravity —kept as accurate as 10^{-5}G for 10 seconds— is generated by 490m-depth free-fall. We developed a system for experiments of free-flyers at the JAMIC. In this paper, we take up two important topics to perform the experiments. The first one is to release a robot stably in the microgravity, and the other is to measure position and orientation of a robot by using cameras set outside of it. Using the experimental system, we performed several experiments of a space robot capturing a target.

1 Introduction

A lot of studies of motion and control of space robots have been carried out theoretically, and at present, realization and operation of space robots in space are investigated by many research groups. Though it is necessary to perform experiments on the ground, the influence of the gravity troubles researchers about credible experiments. One of the methods to simulate a microgravity environment on the ground is using a drop-shaft such as the Japan Microgravity Center (JAMIC). At the center, free-fall of the drop capsule with experimental setups on board generates the microgravity environment as accurate as 10^{-5}G for about 10 seconds. This method has the disadvantage of limited space and time for an experiment and the advantage of a robot free from physical contacts with the surroundings. The former is dominant and therefore there are few studies on experiments in the free-fall environment. Our survey found only the study on nonholonomic motion by Iwata et al.[1]. In the study, the robot is autonomous and has sensors and controllers on board, and therefore it is difficult to miniaturize it or to apply it to other practical experiments such as capturing a target.

The purpose of our research is to establish an experimental system of a space robot in the free-fall environment at the JAMIC. We developed an experimental setup for visual feedback control with two outside cameras and radio remote control. To measure motion of a robot, images of two CCD cameras are processed by the tracking vision system(TRV). In this paper, after describing the outline of the experimental system, we discuss the problem on release of the robot in the microgravity environment, and establish two computational methods to identify the 3D position and orientation of the robot base. The experiments and their results follow to evaluate the developed system.

2 Outline of Microgravity Experiment at the JAMIC

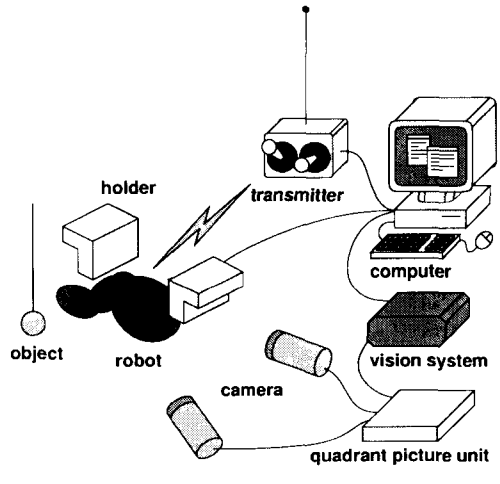

Fig. 1: Experimental System of Visual Feedback Control

The JAMIC has a 710m-depth drop-shaft of which 490m is for free-fall. The drop capsule consists of the inner capsule and the outer one which has a thruster to cancel air drag in falling. The space between them is made a vacuum and the inner capsule falls in the vacuum. Experimental setups are mounted into a

Proc. Fifth International Symposium on Artificial Intelligence, Robotics and Automation in Space, 1-3 June 1999 (ESA SP-440)

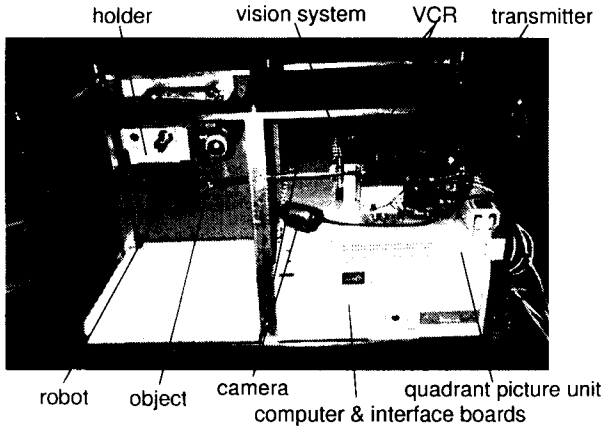

Fig. 2: Assembled Experimental Setup

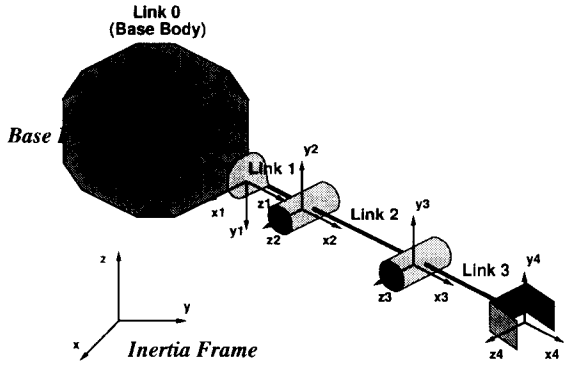

Fig. 3: Experimental Robot with a 3DOF Manipulator

rack which is loaded in the inner capsule. With this system, we can perform experiments in the microgravity environment as accurate as 10^{-5}G for about 10 seconds.

Figure 1 describes our developed setup and it is assembled as shown in Fig.2 to be mounted into the rack. The robot has a 3DOF manipulator which is composed by servo-motors, a receiver, and a battery for radio control. Its mechanism is shown in Fig.3 and its total length is approximately 20cm. The sensors and the controllers are put in the outside of the robot. The two CCD cameras are used for three-dimensional measurement. The images from the cameras enter the 'quadrant picture unit' which is used to arrange the two images into one. The output image of the apparatus is processed by the TRV to compute the position of the target and the position and orientation of the robot. The desired joint angles are designed from these data and transmitted to the robot by radio.

Figure 4 describes the sequence of the experiment. Before drop, the robot is held by the supporting mechanism 'holder' under the gravity. When the

Fig. 4: Experimental Sequence of Capturing a Target

controller receives the drop-start signal from the capsule, the robot is released and starts capturing motion. The sequence is finished when the robot accomplishes capturing the target.

3 Releasing a Robot in Microgravity

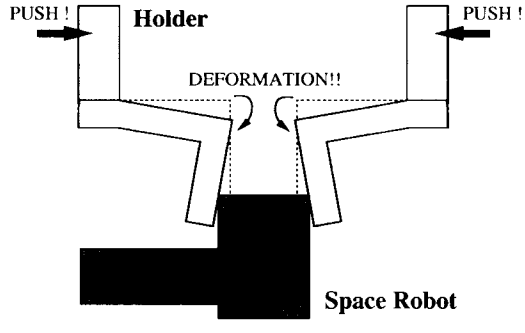

Fig. 5: Deformation of the Supporting Mechanism

One of the critical problems in the microgravity experiment is that the robot suffers force and torque at the contact with the supporting mechanism at the moment of releasing. Large momentum and angular momentum of the robot cause the robot to be

out of control, and therefore it is necessary to keep them small for a stable experiment. In our experiment with the holder shown in Fig.5 which is made of aluminum, we observed the robot moving upward as shown in Fig.6. The cause of the motion is the elastic energy stored in the the holder deformed by the force to support the robot (see Fig.5). To reduce the influence of the elastic energy, we need to choose the shape and material of the holder with high stiffness because elastic energy is inversely proportional to stiffness if holding force is constant. When we designed a sturdy-shaped iron holder, we could release the robot calmly.

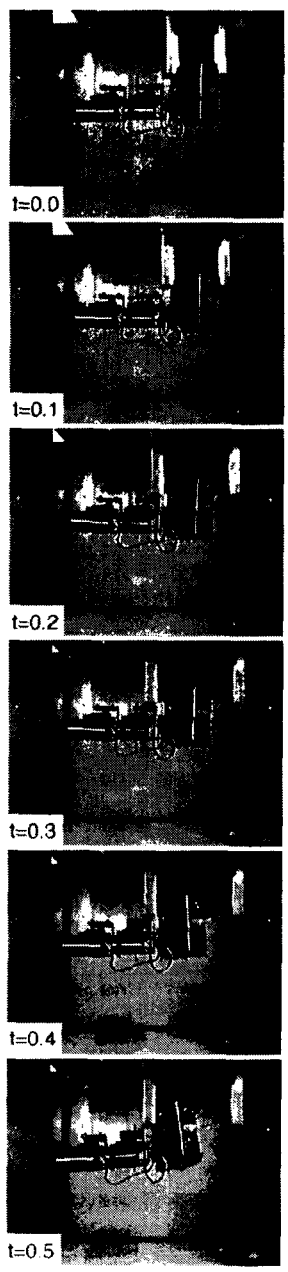

Fig. 6: Upward Motion of the Robot after Released

4 Measurement Methods

The position and orientation of the robot are computed from the data obtained by the TRV processing the images of the two CCD cameras. In this section, we propose two computational methods: (1) stereo-vision method —the 3D positions of plural points marked on the robot base are measured by using the stereo vision and the position and orientation are computed from them—, and (2) non-stereo-vision method —the two cameras observe the different points marked on two surfaces of the robot base respectively and the position and orientation are computed from their images directly, without stereo vision measurement—.

4.1 Stereo-vision Method

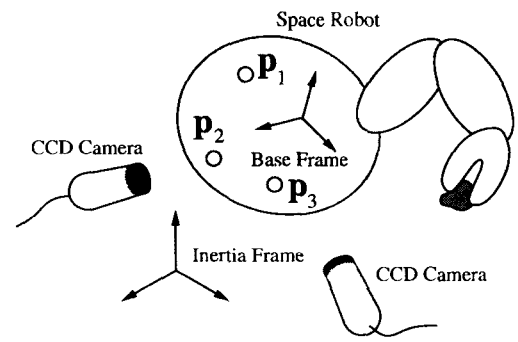

Fig. 7: Two Cameras Looking at the Same Marks

The position and orientation of the robot are computed from the 3D positions of several marks on the base body. The positions of the marks are measured by the stereo vision. The principle of this method is illustrated as follows.

As shown in Fig.7, three points are marked on the surface of the robot base such that they make a triangle. The position of each point in the inertial frame is expressed as follows:

$$ {}^{I}\boldsymbol{p}_i = \boldsymbol{r}_0 + \boldsymbol{R}_0 {}^{b}\boldsymbol{a}_i \qquad (i = 1, 2, 3) \qquad (1) $$

where $\boldsymbol{r}_0$ and $\boldsymbol{R}_0$ denote the position and orientation of the robot base respectively, and ${}^{b}\boldsymbol{a}_i$ the position of each point in the base frame. ${}^{I}\boldsymbol{p}_i$'s are measured by using the stereo vision (see Appendix A). Equation (1) yields the following equations:

$$ {}^{I}\boldsymbol{p}_2 - {}^{I}\boldsymbol{p}_1 = \boldsymbol{R}_0 \left({}^{b}\boldsymbol{a}_2 - {}^{b}\boldsymbol{a}_1 \right) \qquad (2) $$

$$ {}^{I}\boldsymbol{p}_3 - {}^{I}\boldsymbol{p}_1 = \boldsymbol{R}_0 \left({}^{b}\boldsymbol{a}_3 - {}^{b}\boldsymbol{a}_1 \right) \qquad (3) $$

$\boldsymbol{R}_0$ is orthogonal and therefore the following equation is obtained from Eq.(2) and (3).

$$ \left({}^{I}\boldsymbol{p}_2 - {}^{I}\boldsymbol{p}_1 \right) \times \left({}^{I}\boldsymbol{p}_3 - {}^{I}\boldsymbol{p}_1 \right) = \boldsymbol{R}_0 \left\{ \left({}^{b}\boldsymbol{a}_2 - {}^{b}\boldsymbol{a}_1 \right) \times \left({}^{b}\boldsymbol{a}_3 - {}^{b}\boldsymbol{a}_1 \right) \right\} \qquad (4) $$

$\boldsymbol{R}_0$ is computed from Eqs. (2)-(4) which are linearly independent, and $\boldsymbol{r}_0$ is computed by substituting the obtained $\boldsymbol{R}_0$ into Eq.(1).

4.2 Non-stereo-vision Method

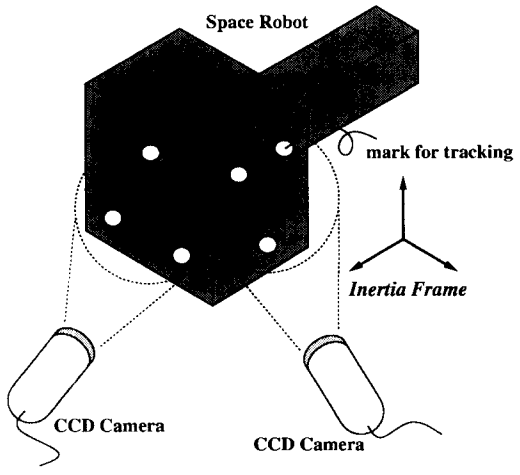

Fig. 8: Two Cameras Looking at the Different Marks

As discussed in the previous section, there is the problem that the holder gives the robot some momentum and angular momentum at the moment of releasing the robot. If the robot rotates and the surface with the marks turns off from the camera vision, it becomes impossible to measure the position and orientation of the robot. In the experiment with the stereo-vision method, the impossibility of measurement occurred as shown in the next section. This problem is inevitable when using such cameras as are set outside of the robot. To expand the measurable region of the robot attitude, we propose the non-stereo-vision method. In the stereo-vision method, the two cameras observe the same marks on the surface of the robot base and therefore the region of the attitude where the marks are simultaneously in the visions of the two cameras is small. In the non-stereo-vision method as shown in Fig.8, the two cameras observe the different points on the two surfaces respectively and therefore the measurable region of the attitude is larger than that of the stereo-vision method.

Three marks for each cameras, altogether six marks, are made on the respective surfaces of the robot base. We call them point-$P_{*i}(* = l, r; i = 1, 2, 3)$. The subscript $*$ represents the left camera or the right one observing the mark. The position of each mark ${}^I\boldsymbol{p}_{*i}$ satisfies the following equation (see Appendix A).

$$\boldsymbol{A}_{*i}\,{}^I\boldsymbol{p}_{*i} = \boldsymbol{b}_{*i} \tag{5}$$

where

$$\boldsymbol{A}_{*i} = \begin{bmatrix} S_{7*}H_{*i} + S_{1*} & S_{8*}H_{*i} + S_{2*} & S_{9*}H_{*i} + S_{3*} \\ S_{7*}V_{*i} + S_{4*} & S_{8*}V_{*i} + S_{5*} & S_{9*}V_{*i} + S_{6*} \end{bmatrix} \tag{6}$$

$$\boldsymbol{b}_{*i} = \begin{bmatrix} H_{*i} - U_{x*} \\ V_{*i} - U_{y*} \end{bmatrix} \tag{7}$$

and $[\ H_{*i}\ V_{*i}\ ]^T$ denotes the position of the point-P_{*i} in the image. The position of each point is expressed as follows:

$${}^I\boldsymbol{p}_{*i} = \boldsymbol{r}_0 + \boldsymbol{R}_0\,{}^b\boldsymbol{a}_{*i} \tag{8}$$

where ${}^b\boldsymbol{a}_{*i}$ denotes the position of the point-P_{*i} with respect to the base frame. Substituting Eq.(8) into Eq.(5), we have

$$\boldsymbol{A}_{*i}\left(\boldsymbol{r}_0 + \boldsymbol{R}_0\,{}^b\boldsymbol{a}_{*i}\right) = \boldsymbol{b}_{*i} \tag{9}$$

where

$$\boldsymbol{r}_0 = [\ r_{01}\ \ r_{02}\ \ r_{03}\ ]^T \tag{10}$$

$$\boldsymbol{R}_0 = \begin{bmatrix} r_{11} & r_{12} & r_{13} \\ r_{21} & r_{22} & r_{23} \\ r_{31} & r_{32} & r_{33} \end{bmatrix} \tag{11}$$

$${}^b\boldsymbol{a}_{*i} = [\ a_{*ix}\ \ a_{*iy}\ \ a_{*iz}\ ]^T \tag{12}$$

Since Eq.(9) is a linear equation of the components of $\boldsymbol{r}_0$ and $\boldsymbol{R}_0$, it is transformed into the following equation:

$$\widetilde{\boldsymbol{A}}\widetilde{\boldsymbol{r}} = \widetilde{\boldsymbol{b}} \tag{13}$$

where

$$\widetilde{\boldsymbol{r}} = [\ r_{01}\ \ r_{02}\ \ r_{03}\ \ r_{11}\ \ r_{12}\ \ r_{13}\ \ r_{21}\ \ r_{22}\ \ r_{23}\ \ r_{31}\ \ r_{32}\ \ r_{33}\ ]^T \tag{14}$$

$$\widetilde{\boldsymbol{b}} = [\ \boldsymbol{b}_{l1}^T\ \ \boldsymbol{b}_{l2}^T\ \ \boldsymbol{b}_{l3}^T\ \ \boldsymbol{b}_{r1}^T\ \ \boldsymbol{b}_{r2}^T\ \ \boldsymbol{b}_{r3}^T\ ]^T \tag{15}$$

and $\widetilde{\boldsymbol{A}}\,(\in R^{12\times 12})$ is easily obtained from Eqs. (6),(7),(9)-(12). From Eq.(13), we can obtain $\widetilde{\boldsymbol{r}}$, that is the components of $\boldsymbol{r}_0$ and $\boldsymbol{R}_0$.

5 Microgravity Experiment

We performed experiments of a space robot capturing a target by using visual feedback control and evaluated our developed experimental system. The results of the experiments with the stereo-vision method and with the non-stereo-vision method are shown in the following.

5.1 With the Stereo-vision Method

Figure 9 shows the images processed by the TRV in the experiment with the stereo-vision method. The left column and the right one show the images of the left camera and the right one respectively. In the

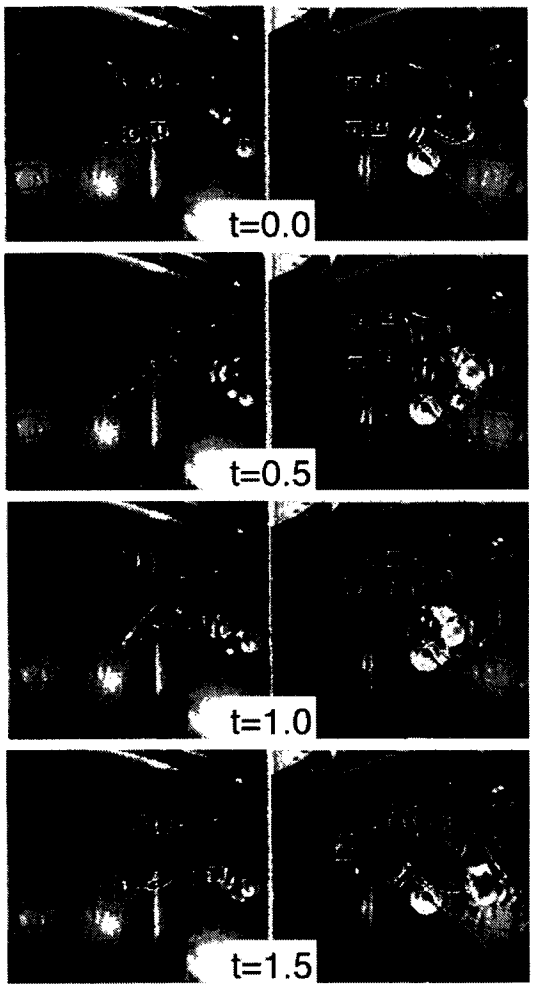

Fig. 9: Motion of the Robot in the Experiment with the Stereo-vision Method

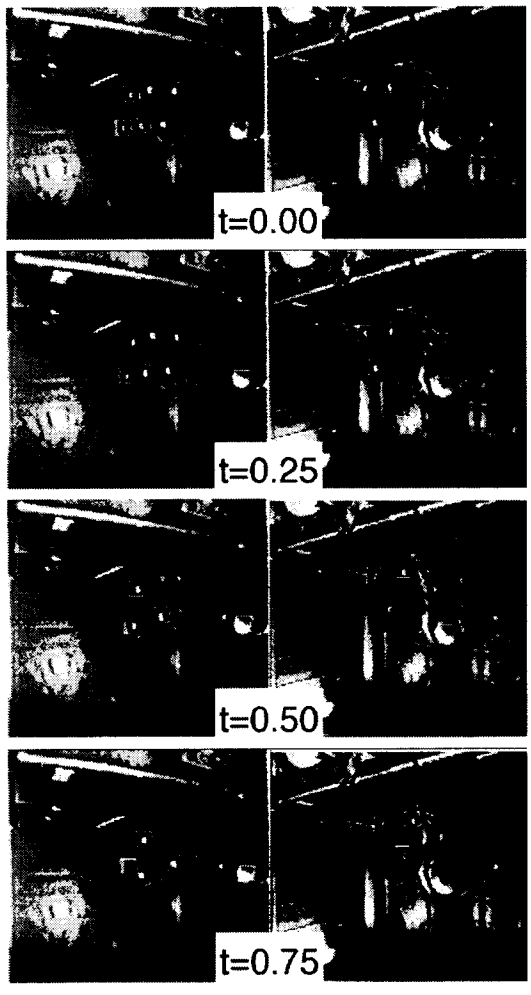

Fig. 10: Motion of the Robot in the Experiment with the Non-stereo-vision Method

figure, the TRV is tracking the images surrounded by the small white squares. After released by the holder, the robot started motion of capturing the target. As mentioned in the previous section, the robot base rotated and the TRV failed tracking the marks just before the robot would accomplish capturing the target. The tip of the arm approached the target steadily and reached just near it.

5.2 With the Non-stereo-vision Method

Figure 10 shows the images processed by the TRV in the experiment with the non-stereo-vision method. the problem of missing the marks didn't occur because of the large measurable region of the robot attitude. The robot accomplished capturing the target as shown in Fig.10.

6 Conclusion

In this paper, we proposed an experimental system in the microgravity environment generated by free-fall, and showed the experiments with the system at the Japan Microgravity Center. We summarize this paper as follows:

1. The microgravity experiment at the JAMIC was explained and the outline of our experimental system was introduced.
2. The problem in releasing the robot stably in the microgravity environment was discussed, and the importance of stiffness of the mechanism supporting the robot was pointed out.
3. We proposed the stereo-vision method and the non-stereo-vision method to measure the position and orientation of the robot.
4. The experimental results with the two proposed measurement methods were shown, and

the problem in measuring motion of the robot by using cameras set outside of the robot was discussed.

References

[1] T.Iwata, K.Kodama, F.Numajiri, and H.Murakami: "Experiment on Robotic Motion Using Drop Shaft," Strengthen Cooperation in the 21 Century (6th ISCOPS) Vol.91, Advances in the Astronautical Society by Univelt, 1996.

[2] Nakamura,Y. and Mukherjee,R., "Formulation and Efficient Computation of Inverse Dynamics of Space Robots", IEEE Trans. on Robotics and Automation, vol.8, no.3, pp.400-406, 1992.

[3] H.Zuang, K.Wang, and Z.S.Roth: Simultaneous Calibration of a Robot and a Hand-Mounded Camera, IEEE Trans. on Robotics and Automation, vol.11, no.5, pp.649-660, 1995.

A 3D Position Measurement

We illustrate the parameters and the computational method used in this paper for measuring the 3D position of a point-P by using two camera, which are based on Ref.[3].

The relation between the position of the point-P in the inertial frame ${}^I\boldsymbol{p}$ and the one in the camera frame ${}^c\boldsymbol{p}$ is expressed as follows:

$$\begin{bmatrix} {}^c\boldsymbol{p} \\ 1 \end{bmatrix} = \begin{bmatrix} \boldsymbol{R} & \boldsymbol{t} \\ \boldsymbol{O}_{1\times 3} & 1 \end{bmatrix} \begin{bmatrix} {}^I\boldsymbol{p} \\ 1 \end{bmatrix} \tag{16}$$

where

$$ {}^I\boldsymbol{p} = [\ x_I \quad y_I \quad z_I\ ]^T \tag{17}$$

$$ {}^c\boldsymbol{p} = [\ x_c \quad y_c \quad z_c\ ]^T \tag{18}$$

$$ \boldsymbol{R} = \begin{bmatrix} r_1 & r_2 & r_3 \\ r_4 & r_5 & r_6 \\ r_7 & r_8 & r_9 \end{bmatrix} \tag{19}$$

$$ \boldsymbol{t} = [\ t_x \quad t_y \quad t_z\ ]^T \tag{20}$$

${}^c\boldsymbol{p}$ is transformed to the two-dimensional coordinates in the image plane by perspective as follows:

$$\frac{x_v}{f} = \frac{x_c}{z_c}, \qquad \frac{y_v}{f} = \frac{y_c}{z_c} \tag{21}$$

where $[\ x_v\ y_v\ ]^T$ denote the position of the point-P in the image plane and f the focal distance of the camera. The transformation from the pixel unit to the unit of the inertia coordinates is expressed as:

$$s_x x_v = H - c_x\ , \qquad s_y y_v = c_y - V \tag{22}$$

where $[\ H\ V\ ]^T$ denotes the pixel-unit position of the point-P on the image, $[\ c_x\ c_y\ ]^T$ that of the image center, and s_x, s_y the camera scale factors. From Eqs.(16)-(22), we obtain

$$\boldsymbol{C}\boldsymbol{\phi} = 0 \tag{23}$$

where

$$\boldsymbol{C} = \begin{bmatrix} x_I & 0 & x_I H & y_I & 0 & y_I H \\ 0 & x_I & x_I V & 0 & y_I & y_I V \\ & & & z_I & 0 & z_I H & 1 & 0 & H \\ & & & 0 & z_I & z_I V & 0 & 1 & V \end{bmatrix} \tag{24}$$

$$\boldsymbol{\phi} = [\ S_1 \quad S_4 \quad S_7 \quad S_2 \quad S_5 \quad S_8 \quad S_3 \quad S_6 \quad S_9 \quad U_x \quad U_y \quad -1\ ]^T \tag{25}$$

$$\left.\begin{array}{ll} S_1 = \frac{s_x f r_1 + c_x r_7}{t_z} & S_2 = \frac{s_x f r_2 + c_x r_8}{t_z} \\ S_3 = \frac{s_x f r_3 + c_x r_9}{t_z} & S_4 = -\frac{s_y f r_4 - c_y r_7}{t_z} \\ S_5 = -\frac{s_y f r_5 - c_y r_8}{t_z} & S_6 = -\frac{s_y f r_6 - c_y r_9}{t_z} \\ S_7 = -\frac{r_7}{t_z} \quad S_8 = -\frac{r_8}{t_z} & S_9 = -\frac{r_9}{t_z} \\ U_x = \frac{s_x f t_x + c_x t_z}{t_z} & U_y = -\frac{s_y f t_y - c_y t_z}{t_z} \end{array}\right\} \tag{26}$$

$\boldsymbol{\phi}$ consists of the unknown camera parameters and therefore is decided by the camera calibration. We define the parameters for the two cameras as follows:

$$\boldsymbol{\phi}_* = [\ S_{1*} \quad S_{4*} \quad S_{7*} \quad S_{2*} \quad S_{5*} \quad S_{8*} \quad S_{3*} \quad S_{6*} \quad S_{9*} \quad U_{x*} \quad U_{y*} \quad -1\ ]^T \quad (* = l, r) \tag{27}$$

The pixel unit positions of the point-P on the two images are represented by $[\ H_l\ V_l\ ]^T$ and $[\ H_r\ V_r\ ]^T$ respectively. Then, ${}^I\boldsymbol{p}$ is computed from the following equation.

$$\boldsymbol{A}\,{}^I\boldsymbol{p} = \boldsymbol{b} \tag{28}$$

where

$$\boldsymbol{A} = \begin{bmatrix} S_{7l}H_l + S_{1l} & S_{8l}H_l + S_{2l} & S_{9l}H_l + S_{3l} \\ S_{7l}V_l + S_{4l} & S_{8l}V_l + S_{5l} & S_{9l}V_l + S_{6l} \\ S_{7r}H_r + S_{1r} & S_{8r}H_r + S_{2r} & S_{9r}H_r + S_{3r} \\ S_{7r}V_r + S_{4r} & S_{8r}V_r + S_{5r} & S_{9r}V_r + S_{6r} \end{bmatrix} \tag{29}$$

$$\boldsymbol{b} = \begin{bmatrix} H_l - U_{xl} \\ V_l - U_{yl} \\ H_r - U_{xr} \\ V_r - U_{yr} \end{bmatrix} \tag{30}$$